

Transmission Line Boundary Protection Using Wavelet Transform and Neural Network

Nan Zhang, *Student Member, IEEE*, and Mladen Kezunovic, *Fellow, IEEE*

Abstract—Two of the most expected objectives of transmission line protection are: a) differentiating precisely the internal faults from external, and b) indicating exactly the fault type using one end data only. This paper proposes an improved solution based on wavelet transform and self-organized neural network. The measured voltage and current signals are preprocessed first and then decomposed using wavelet multi-resolution analysis to obtain the high frequency details and low frequency approximations. The patterns formed based on high frequency signal components are arranged as inputs of neural network #1, whose task is to indicate whether the fault is internal or external. The patterns formed using low frequency approximations are arranged as inputs of neural network #2, whose task is to indicate the exact fault type. The new method uses both low and high frequency information of the fault signal to achieve an advanced line protection scheme. The proposed approach is verified using frequency-dependent transmission line model and the test results prove its enhanced performance. A discussion of the application issues for the proposed approach is provided at the end where the generality of the proposed approach and guidance for future study are pointed out.

Index Terms—Adaptive resonance theory, boundary protection, fault classification, neural network, pattern recognition, power system faults, power system protection, wavelet transform.

I. INTRODUCTION

A perfect transmission line protection scheme is expected to: a) differentiate the internal faults from external precisely so that only the faulted line will be removed; b) provide the exact fault type selection so that advanced single-pole tripping and reclosing schemes can be implemented. The reliability of those two functions is highly desirable so that the impact of faults on system stability is reduced.

The traditional line protection schemes based on fundamental frequency components of the fault generated transient voltage and current signals, can be classified into two categories: a) non-unit protection and b) unit protection. The non-unit protection schemes use one end transmission line data while the unit protection schemes usually use data from two ends. The non-unit protection such as distance relay, can not protect the entire length of the primary line because it can not differentiate the internal faults from external occurring around the multi-zone boundaries. Backup protection may be introduced as a trade-off approach for protecting the entire

length of the transmission line. For unit protection such as pilot protection, it usually requires a communication link to transmit the blocking or transfer tripping signals. Therefore, the reliability of the protection scheme highly relies on the reliability of the communication link. The cost of the communication link also needs to be taken into account.

Recently, new techniques using high frequency components of the fault generated transient signals were studied and some useful solutions were obtained [1]–[4]. An approach called “boundary protection” for solving the disadvantages of conventional non-unit protection schemes was proposed [2], [5]. This approach introduces a possibility of precisely differentiating the internal faults from external using data from one end only. In this case, the relay at one end can protect the entire line length with no intentional time delay.

Regarding the fault type selection or classification, the traditional method is based on the fundamental frequency phasors. The feature formed by a nonlinear ratio between voltage and current phasors is compared to the threshold to find out the faulted phase [6]. This kind of method is affected by the different conditions such as remote-end infeed, fault resistance, mutual coupling of parallel lines, etc. An alternate solution is to use artificial intelligence schemes such as neural network based algorithm [7], [8].

This paper introduces a new approach based on wavelet transform and a self-organized neural network to realize accurate boundary protection and fault type classification using one end transmission line data. The new method retains both low frequency and high frequency component of the fault signal to achieve high reliability and selectivity of the protection scheme. It inherits many advantages from different techniques it utilizes.

The paper first presents, in Section II, the background of boundary protection. Brief introduction of wavelet transform and self-organized neural network algorithm are then provided in Section III and Section IV respectively. Section V describes the entire design procedure of the new protection scheme, followed by a performance study in Section VI. A discussion of the application issues for the proposed approach is provided in Section VII. Conclusion of the paper is summarized at the end.

II. BACKGROUND OF BOUNDARY PROTECTION

The principle of boundary protection was studied in [2]. The previous work is explored in this section to provide background of the new approach introduced in this paper. The system shown in Fig. 1 is a typical multi-line system. We

This work was supported by NSF IUCRC Power Systems Engineering Research Center (PSerc), project S-19 titled “Detection, Prevention and Mitigation of Cascading Events”.

N. Zhang and M. Kezunovic are with the Department of Electrical and Computer Engineering, Texas A&M University, College Station, TX 77843-3128, USA (e-mails: zhangnan@tamu.edu, kezunov@ece.tamu.edu).

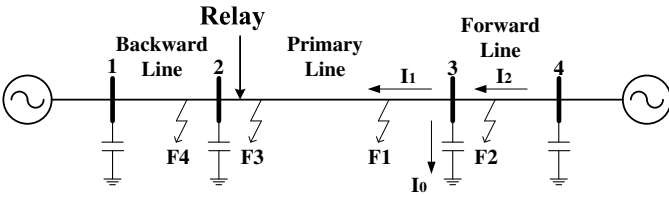


Fig. 1. A typical multi-line system

assume the relay is installed at the bus 2 to protect the line 2 – 3 shown in the figure. A fault on the lines will generate wideband transient voltage and current signals. The signals will travel in both directions with reflections and refractions at the discontinuity points, which are usually the buses and faults. The bus of the power system is always connected to many power system apparatus and they usually represent the capacitance at high frequency. This effect is shown in Fig. 1. For an external fault $F2$ close to the bus 3, the high frequency portion of the fault current signal I_2 will be shunted to earth (in I_0) significantly due to the bus capacitance. The higher the frequency, the more significant portion of the current signal will be shunted. From the viewpoint of the relay, the magnitude of high frequency portion of the fault current signal I_1 is reduced. In contrast, for the internal fault $F1$ close to the bus 3, the fault current of the entire frequency band can be seen by the relay. That means, if other fault conditions (fault type, fault resistance, fault angle) are identical, we can differentiate the internal fault $F1$ from the external fault $F2$ by comparing the high frequency portions of their signals. Similarly, the same method can be used to differentiate the faults at $F3$ and $F4$. Using the voltage signals, we can still differentiate faults at $F1$ and $F2$ but can not differentiate faults at $F3$ and $F4$ because the voltage measurements of the relay are obtained from bus 2.

The feature differences of the faults on different line sections seen by the relay at bus 2 in Fig. 1 can be summarized as follows:

- For faults on the primary line, the energy of high frequency portion of the voltage and current signals will be seen as “big” values.
- For faults on the backward line, the energy of high frequency portion of the voltage signals will be seen as “big” values while the energy of high frequency portion of the current signals will be seen as “small” values.
- For faults on the forward line, the energy of high frequency portion of the voltage and current signals will be seen as “small” values.

It should be emphasized that the above statements are based on the assumption that all other fault parameters are the same and the “big” and “small” value are indicating relative numbers. The absolute values are dependent on fault type, fault resistance, fault angle, etc.

In [2], the author uses a specially designed multi-channel filter to extract the transient current signals for two signal outputs I_{f1} , I_{f2} with center frequency at $80kHz$ and $1kHz$ respectively. Then the ratio of the energy spectrum for I_{f1} , I_{f2} is calculated and compared to a threshold to find out whether

the fault is internal or external. The advantage of this method is justified by the result from a performance study.

Still some issues are remaining in this method: a) The direction of the external faults can not be distinguished since only the current signal is used. The method also has no phase selection function available; b) The theoretical basis for selection of the center frequency of the extracted features and selection of the thresholds is not apparent; c) The reliability of the method is unknown since only high frequency signal is used. It may be affected by the disturbance from noise, switching, lightning, etc; d) There are no extensive studies provided for the performance evaluation under various fault conditions. As mentioned earlier, the boundary condition are highly dependent on fault type, fault resistance, fault angle, etc.

This paper provides a new boundary protection scheme aimed at solving those issues. First of all, the voltage and current signal will both be used; this can provide more information about the direction of the fault point. The new scheme uses wavelet transform as the feature extraction tool thus there is no need to design extra filters. Wavelet transform has a strong capability of extracting the signal component under different frequency bands while retaining the time domain information. Secondly, the extracted features will be handled using a self-organized neural network algorithm [7]. With its strong capability of generalization and training mechanism, it can be used as an alternative solution when theoretical basis for dealing with the fault generated high frequency signal components is not well defined. The neural network based algorithm is also capable of implementing a superior fault classification scheme. Finally, the new scheme will use both the low and high frequency components of the fault signal to eliminate impact from non-fault disturbances. The reliability and robustness of the method will be verified by an extensive study for various kinds of faults.

III. WAVELET TRANSFORM

Wavelet analysis is a relatively new signal processing tool and is applied recently by many researchers in power systems due to its strong capability of time and frequency domain analysis [9], [10]. The two areas with most applications are power quality analysis and power system protection [11]–[13].

The definition of continuous wavelet transform (CWT) for a given signal $x(t)$ with respect to a mother wavelet $\psi(t)$ is:

$$CWT(a, b) = \frac{1}{\sqrt{a}} \int_{-\infty}^{\infty} x(t) \psi\left(\frac{t-b}{a}\right) dt \quad (1)$$

where a is the scale factor and b is the translation factor.

For CWT, t , a , b are all continuous. Unlike Fourier transform, the wavelet transform requires selection of a mother wavelet for different applications. One of the most popular mother wavelets found for power system transient analysis in the literature is Daubichies’s wavelet family. In this paper, the $db5$ wavelet is selected as the mother wavelet for detecting the short duration, fast decaying fault generated transient signals.

The application of wavelet transform in engineering areas usually requires discrete wavelet transform (DWT), which

implies the discrete form of t , a , b in (1). The representation of DWT can be written as:

$$DWT(m, n) = \frac{1}{\sqrt{a_0^m}} \sum_k x(k) \psi \left(\frac{k - nb_0 a_0^m}{a_0^m} \right) \quad (2)$$

where original a and b parameters in (1) are changed to be the functions of integers m , n . k is an integer variable and it refers to a sample number in an input signal.

A very useful implementation of DWT, called multi-resolution analysis, is demonstrated in Fig. 2. The original sampled signal $x(n)$ is passed through a highpass filter $h(n)$ and a lowpass filter $l(n)$. Then the outputs from both filters are decimated by 2 to obtain the detail coefficients and the approximation coefficients at level 1 ($D1$ and $A1$). The approximation coefficients are then sent to the second stage to repeat the procedure. Finally, the signal is decomposed at the expected level. In the case shown in Fig. 2, if the original sampling frequency is F , the signal information captured by $D1$ is between $F/4$ and $F/2$ of the frequency band. $D2$ captures the information between $F/8$ and $F/4$. $D3$ captures the information between $F/16$ and $F/8$, and $A3$ retains the rest of the information of original signal between 0 and $F/16$. By such means, we can easily extract useful information from the original signal into different frequency bands and at the same time the information is matched to the related time period. An example, given in Fig. 3, illustrates the procedure. The original signal is one cycle of a post-fault current signal, as shown in Fig. 3 (a). We use $db5$ wavelet to make a 5 level decomposition. The reconstructed versions of each detail and the approximation are shown in Fig. 3 (b). The information of original signal is clearly represented at each frequency band. The original signal can be reconstructed by adding up those wavelet signals at the same sample point. The wavelet toolbox in MATLAB provides a lot of useful techniques for wavelet analysis [14].

IV. SELF-ORGANIZED ART NEURAL NETWORK ALGORITHM

The traditional transmission line protection schemes are mostly based on calculation of certain electric values and their comparison to pre-defined thresholds. This kind of method relies on a “hard” criterion. The settings require complex system analysis to cover worst case fault conditions. This method can only consider one criterion at a time, hence the flexibility is limited. The threshold based algorithm needs extensive theoretical analysis and verification through elaborate field evaluations.

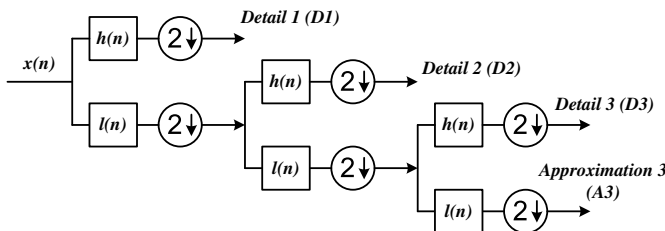


Fig. 2. Wavelet multi-resolution analysis

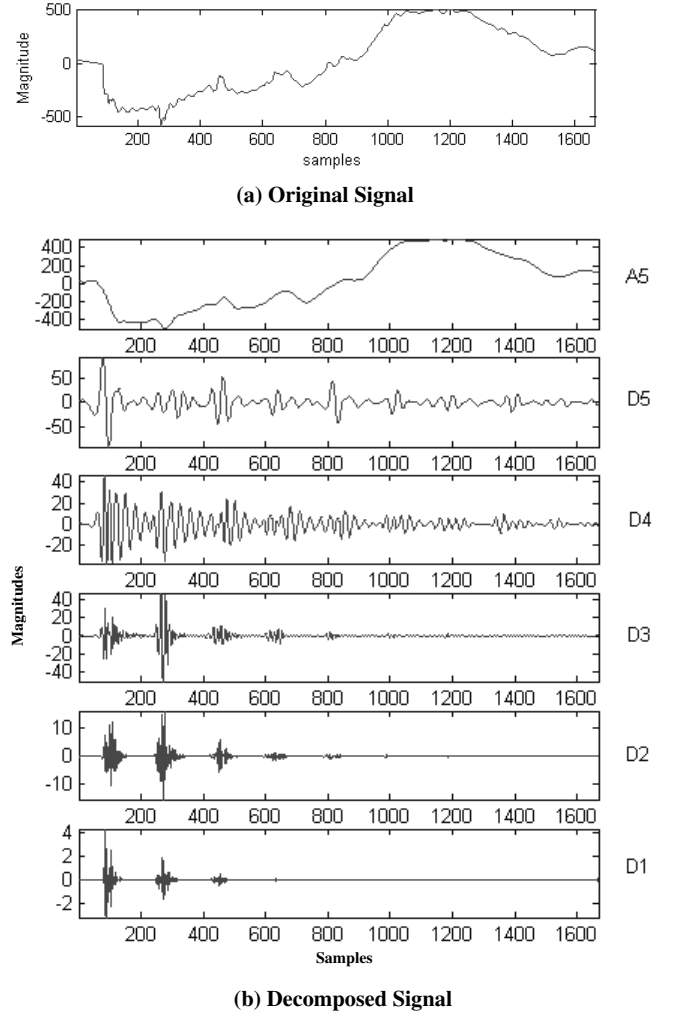


Fig. 3. An example of wavelet multi-resolution analysis

The above issues can be avoided by applying a “soft” criterion based on artificial intelligence techniques. Neural network is such a technique and has been studied in the power system area for quite a while [15]–[17]. Its major advantage is that it can take into account several features of the input signals simultaneously and compare the patterns according to their mutual similarity instead of the “hard” thresholds.

There are several types of neural networks used for power system protection. The multi-layer perceptron (MLP) neural network with back propagation (BP) algorithm is the one that was dominantly used in the power system studies since it can be easily realized. Dealing with large input set, selecting the number of hidden neurons, and facing the convergence problem are the inherent issues when applying MLP neural networks.

In this paper, a type of self-organized, adaptive resonance theory (ART) neural network [18] is used. The prototype of this algorithm is described in [7]. The scheme is illustrated briefly here and more details can be found in [7].

A 2-D example is shown in Fig. 4. The raw input patterns belonging to two categories are presented in a normalized 2-D space as shown in Fig. 4 (a). The objective of neural network

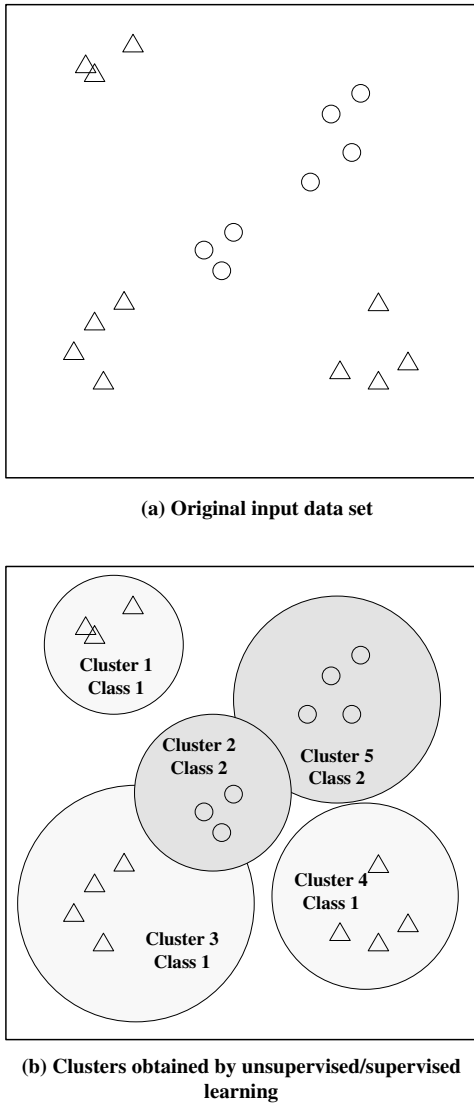


Fig. 4. An example of training mechanism of adopted neural network algorithm

training is to allocate the input data into several prototype clusters that belong to same categories or classes according to their mutual similarity, as shown in Fig. 4 (b).

The neural network training uses a mechanism of clustering technique with combined unsupervised and supervised learning. The architecture is shown in Fig. 5.

Unsupervised learning is the first stage aimed at processing the raw data set. During this stage, the category of each pattern is not presented in advance. The input patterns are grouped by themselves according to their mutual similarity. Neither the initial guess of the number of cluster nor their position is specified in advance. Unsupervised learning consists of two steps: initialization and stabilization. In initialization phase, the entire pattern set is presented only once to establish initial cluster structure based on similarity between patterns. The Euclidean distances between patterns are measured and compared to the current threshold (radius of the cluster) to decide whether they belong to same clusters. In stabilization phase, the entire pattern set is being presented numerous times

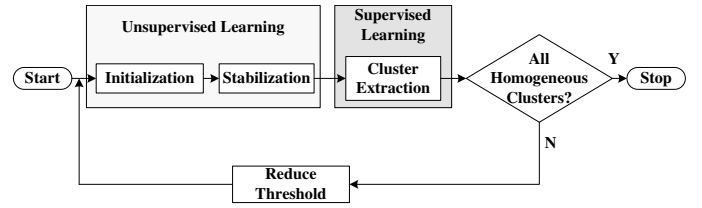


Fig. 5. The architecture of neural network training

and the process is similar to that in initialization phase. The iterations will not end until the initial unstable cluster structure becomes stable and no patterns change clusters after a single iteration.

During supervised learning, class label is assigned to each input pattern allowing separation of homogenous (all patterns belong to same class) and non-homogenous clusters produced in unsupervised learning. For homogeneous clusters, their position, size, and category are stored into the memory and the patterns from those clusters are removed from current training pattern set. The remaining patterns, presented in non-homogenous clusters, are left for new learning iterations. When all clusters are examined, the new data set is sent to next unsupervised/supervised learning iteration with reduced threshold, as shown in Fig. 5. The entire learning process is completed when all the patterns are grouped into homogeneous clusters with predefined class labels.

The advantage of this kind of neural network is that the number of clusters is increased and their positions are updated automatically during the learning, and there is no need to define them in advance. This is the reason why the selection of the number of hidden neurons is not an issue in this method. Regarding large data set and convergence issue, the data set can be separable no matter how many input data are presented since the size of the clusters can be reduced infinitely during training.

The prototypes of trained clusters are used for on-line detection of unknown patterns. If the new pattern falls in the sphere of a cluster, the pattern is assigned to the category that cluster belongs to. If the new pattern falls in an unclaimed area, fuzzy K-nearest neighbor (K-NN) algorithm [19] is used for assigning its category by taking into account the influence of surrounding clusters.

V. DESIGN OF THE NEW PROTECTION SCHEME

A. Overview of the Scheme

The framework of the entire protection scheme is shown in Fig. 6. We assume that standard design of an intelligent electronic device (IED) can be adjusted to meet the requirement of the proposed scheme.

The three-phase secondary voltage and current signals shown in Fig. 6 are obtained at the sampling rate of $200kHz$. The zero-sequence voltage and current are obtained by adding up the phase values. Through the signal preprocessing stage, the pre-fault steady state component is removed from each signal. Then the wavelet multi-resolution analysis is used for decomposing each signal into low frequency approximation

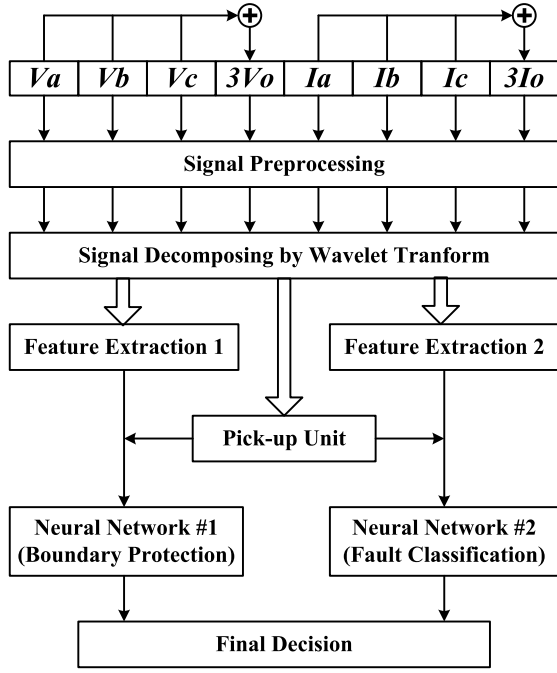


Fig. 6. Overview of proposed protection scheme

and high frequency details. The information is used for extracting the features and forming the patterns for neural network algorithm. Two neural networks are trained to handle the boundary protection and fault classification respectively. The final conclusion can be made by simultaneously combining the conclusions of the two neural networks and then appropriate actions should be issued by the relay. A pick-up unit is introduced before the neural network algorithms as a threshold to screen the non-fault disturbances in low frequency band (such as overload, power swing, etc.) and in high frequency band (such as noise, switching, lightning, etc.).

B. Signal Preprocessing

To reduce the impact from the pre-fault load and only consider the post-fault abrupt variation of voltage and current waveforms, a simple signal preprocessing method is used as follows [20]:

$$\begin{aligned} i(k) &= i(k) - i(k-n); \\ v(k) &= v(k) - v(k-n) \end{aligned} \quad (3)$$

where k represents the sample number at the current measuring point and n represents the number of samples in one cycle.

By this approach, the pre-fault steady state components are removed from the observed measurements. When there is no fault, the obtained voltage and current samples from (3) are close to zero (normal state), or small values (under power swing). When there is a fault, the fault-generated transient values are observed clearly.

C. Feature Extraction

The features used as inputs of the neural network are extracted from half cycle of samples in a sliding window. At

every time step after preprocessing stage, the eight-channel signals are sent to the wavelet transform stage. Using the scheme shown in Fig. 2, the signals are decomposed using $db5$ wavelet to level 5. Since the sampling rate is $200kHz$, the obtained coefficients $A5, D5, D4, D3, D2$ and $D1$ correspond to the frequency band of $0-3.125kHz, 3.125-6.25kHz, 6.25-12.5kHz, 12.5-25kHz, 25-50kHz, 50-100kHz$ respectively. Those values are used for feature extraction in the pick-up unit and in the neural networks.

For the pick-up unit, the purpose is to avoid the non-fault disturbances. The method is flexible and easy to realize. For instance, we can compare the energy spectra of the approximation $A5$ and the detail $D3$ of three-phase currents with the pre-defined thresholds, as shown in (4). If the condition is met in any phase, the boundary detection and fault classification are activated.

$$[E(A_5) > Threshold_1] \& [E(D_3) > Threshold_2] \quad (4)$$

where

$$\begin{aligned} E(A_5) &= \sum_{k=1}^m I_{p-app-A5}^2(k)\Delta t; & p = a, b, c \\ E(D_3) &= \sum_{k=1}^m I_{p-det-D3}^2(k)\Delta t; & p = a, b, c \end{aligned}$$

$I_{p-app-A5}$ and $I_{p-det-D3}$ represent the wavelet signals at $A5$ and $D3$ respectively, as shown in Fig. 3.

Δt is the time step for the samples. m is the number of total samples in a data window.

The pattern arranged for boundary protection is shown in Fig. 7 (a). For that pattern, there are four features obtained for one of the phase voltages and currents. Therefore the pattern dimension is 24×1 . The four features in each phase are defined as follows:

$$\begin{aligned} x_1 &= \log [E(D_1) / E(D_5)] \\ x_2 &= \log [E(D_1) / E(D_4)] \\ x_3 &= \log [E(D_2) / E(D_5)] \\ x_4 &= \log [E(D_2) / E(D_4)] \end{aligned} \quad (5)$$

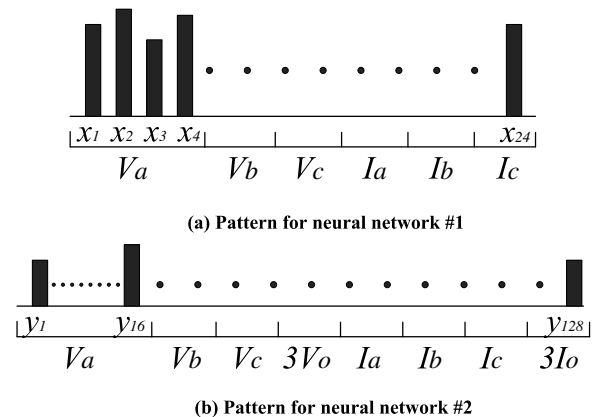


Fig. 7. Pattern arrangement for two neural networks

where $E(D_x)$ is the energy spectrum at detail x and the definition is the same as in (4).

The reason for this arrangement is explained next. As mentioned in Section II, the main feature differences between the external faults and internal faults are preserved in their high frequency components. The higher the frequency, the more prominent the feature difference. Therefore, the energy spectra of higher frequency details are taken as the main features. The absolute values of the energy spectra of higher frequency details are strongly dependent on different fault type, fault resistance and fault angles, etc. To reduce that influence, the energy spectra of the lower frequency details are taken as the reference. If only one high frequency detail and one low frequency detail are used, it is easy to lose the robustness and the redundant information obtained by wavelet transform is wasted. As shown in (5), we take the two highest frequency details as main features and the two lowest frequency details as references.

The pattern arranged for fault classification is shown in Fig. 7 (b). For that pattern, there are 16 features per phase obtained in half cycle of voltage or current signals. The zero-sequence voltage and current are also taken into account for indicating whether the ground is involved during the fault. The entire input pattern dimension is 128×1 . The features are the samples decimated through the approximation coefficients:

$$(y_1, \dots, y_{16}) = \text{Decimated}[\text{Coef}(A_5)] \quad (6)$$

The neural network based fault classification using raw voltage and current samples was studied in [7]. The performance is very good but the following problems still exist: a) the algorithm may be influenced by the system operating conditions and power swing; b) by combining fault zone detection, the performance will be degraded. The first problem is solved here by introducing the signal preprocessing stage. For the second problem, since the neural network #1 handles the task to differentiate the internal faults from external, neural network #2 can focus on the fault events on the line of interest only. The number of both inputs and outputs for neural network training is reduced. Hence the accuracy of fault classification will be improved significantly.

D. Neural Network Training and Testing

The final stage of this scheme is to train and test the two neural networks using simulated fault scenarios. The field recordings could be used as additional scenarios to calibrate the neural network training. Thousands of fault scenarios could be generated taking into account the different fault types, locations, resistances and inception angles. For a single scenario, two corresponding patterns as shown in Fig. 7 are formed for the two neural networks respectively. Both of the networks form their pattern prototypes (clusters) during the training. The neural networks are then tested by another data set. If the performance is acceptable, the solution can be used online.

It should be noted that the patterns shown in Fig. 7 (a) and Fig. 7 (b) need to be normalized into the range of $[-1, 1]$

before the training and testing process. A general equation is defined as:

$$p = 2 \times [p - \min(p)] / [\max(p) - \min(p)] - 1 \quad (7)$$

where $\min(p)$ and $\max(p)$ are the minimum and maximum values of the entire input space of feature p .

For neural network #1, the $\min(p)$ and $\max(p)$ must be found individually for each feature, and they are defined as:

$$\begin{aligned} \min(x_i) &= \min[x_{1i}, \dots, x_{ki}]; \\ \max(x_i) &= \max[x_{1i}, \dots, x_{ki}] \end{aligned} \quad (8)$$

where k represents the number of the training patterns.

For neural network #2, only four $\min(p)$ and $\max(p)$ are needed. Equation (9) gives the pairs for features of phase voltages $y_i(V_a, V_b, V_c)$. The values for $y_i(3V_0)$, $y_i(I_a, I_b, I_c)$ and $y_i(3I_0)$ are calculated in a similar way.

$$\begin{aligned} \min[y_i(V_a, V_b, V_c)] &= \min \begin{bmatrix} y_{1,1}(V_a), & \dots, & y_{k,16}(V_a) \\ y_{1,1}(V_b), & \dots, & y_{k,16}(V_b) \\ y_{1,1}(V_c), & \dots, & y_{k,16}(V_c) \end{bmatrix} \\ \max[y_i(V_a, V_b, V_c)] &= \max \begin{bmatrix} y_{1,1}(V_a), & \dots, & y_{k,16}(V_a) \\ y_{1,1}(V_b), & \dots, & y_{k,16}(V_b) \\ y_{1,1}(V_c), & \dots, & y_{k,16}(V_c) \end{bmatrix} \end{aligned} \quad (9)$$

VI. PERFORMANCE STUDIES

A. Power System Model

The performance studies in this paper are based on the 500kV power system model shown in Fig. 8. The system is modeled using alternative transient program (ATP) [21], where the three transmission lines are J. Marti frequency-dependent models created in ATP-LCC subroutine in order to observe the frequency effects more accurately. The lengths of the three lines are set identically to 200 miles for simplicity. The bus capacitances are set identically to $0.1\mu F$, which is the typical value from the literature.

B. Feature Comparison

This section will give some examples of feature comparison from different fault scenarios.

For the boundary protection, six fault points are selected for comparison, as shown in Fig. 8. Those fault points are located 5 miles away from the nearest bus. For illustration, we randomly selected an ABG fault, with fault resistance of 10Ω and fault angle of 70° identical for all six fault points. If the six fault scenarios form the entire input space, we can

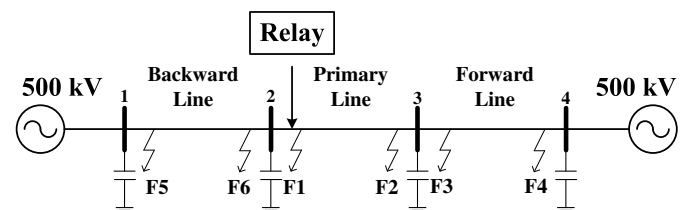


Fig. 8. The studied multi-line system

obtain the patterns for boundary protection (neural network #1) as shown in Fig. 9.

The arrangement for each pattern is the same as the one shown in Fig. 7 (a). The first half represents the voltage features and the second half represents the current features. Comparatively, the internal faults at $F1$ and $F2$ have higher values for both voltage and current features. The forward faults at $F3$ and $F4$ have smaller value for both voltage and current features. The backward line faults at $F5$ and $F6$ have higher value for voltage features and smaller value for current features. The effect is much clearer for the fault point pairs ($F1$ and $F6$, $F2$ and $F3$) located on opposite side of the same bus. Those results confirm the conclusions in section II, which means the faults on different line sections are clearly differentiable.

At $F1$, a set of scenarios including all fault types is generated to demonstrate the features for fault type classification. The fault resistance and fault angle are also selected as 10Ω and 70° respectively. The patterns of all fault types for neural network #2 are shown in Fig. 10. The arrangement for each pattern is the same as the one shown in Fig. 7 (b). As can be seen, the waveform is clearly presented only for the phases involving the fault. In that case, all the fault types are also easily differentiable by this pattern arrangement approach.

C. Neural Network Training

We generated a set of 3960 fault scenarios for the system shown in Fig. 8 using interactively ATP and MATLAB [22] as simulation tools for training the neural networks. On each line section, there are 1320 fault cases taking into account all the fault types, five fault locations at 2.5, 50, 100, 150, 197.5 miles from the bus at the left-hand side, several fault resistances in

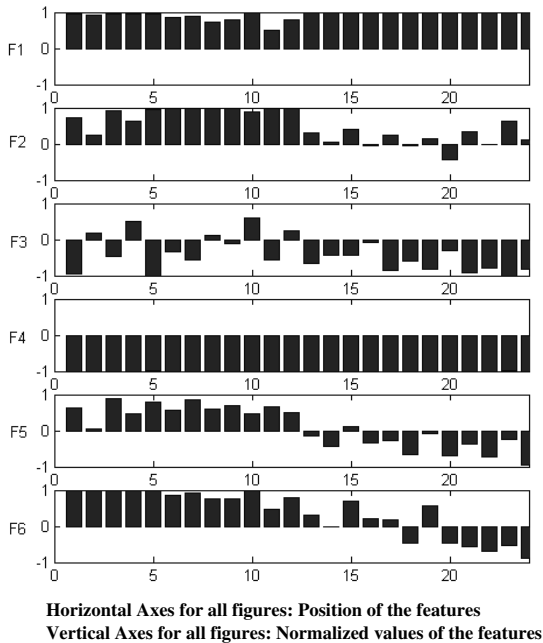


Fig. 9. Pattern comparison for boundary protection (neural network #1)

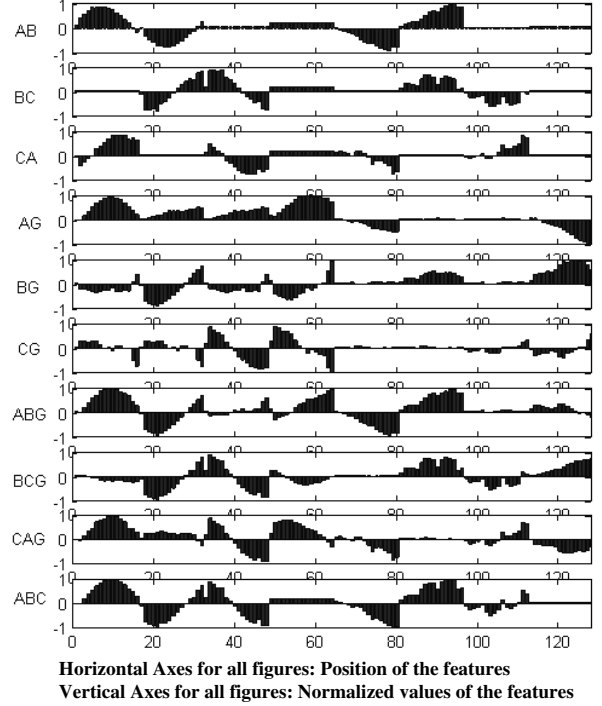


Fig. 10. Pattern comparison for fault classification (neural network #2)

the range of $0 - 100\Omega$, and several fault angles in the range of $0 - 180^\circ$.

For neural network #1, all 3960 cases are used as inputs for training. The outputs of the neural network are “Normal”, “Primary line fault”, “Forward line fault” and “Backward line fault”. For a comparison, we select two features from the input pattern of the entire 3960 cases to compare the feature differences, as shown in Fig. 11. The meaning of those two features for each pattern can be found using Fig. 7 (a) and equation (5). We can see that in general, the features from different line sections can easily be differentiated since they are generally distributed in different ranges. We can also see that there are also some spikes observed for voltage and current features. Those spikes are primarily due to some abnormal ratios of high/low frequency component of fault signals in the un-faulted phase. For example, for a B-C fault, the “ $x1$ ” feature in Phase A could be an abnormal spike since there is nearly no high frequency component in each frequency band. The neural network training can tolerate the abnormal feature since all of the features in three phases will be taken into account by the training process. That is where we can benefit from the neural network algorithm to deal with the problem. If those exceptions do not exist, we can use “hard” thresholds directly for the boundary protection.

For neural network #2, only 1320 fault cases on the primary line are used as the inputs for training since only the events on the primary line are of concern in this case. The outputs of neural network #2 indicate the fault type directly.

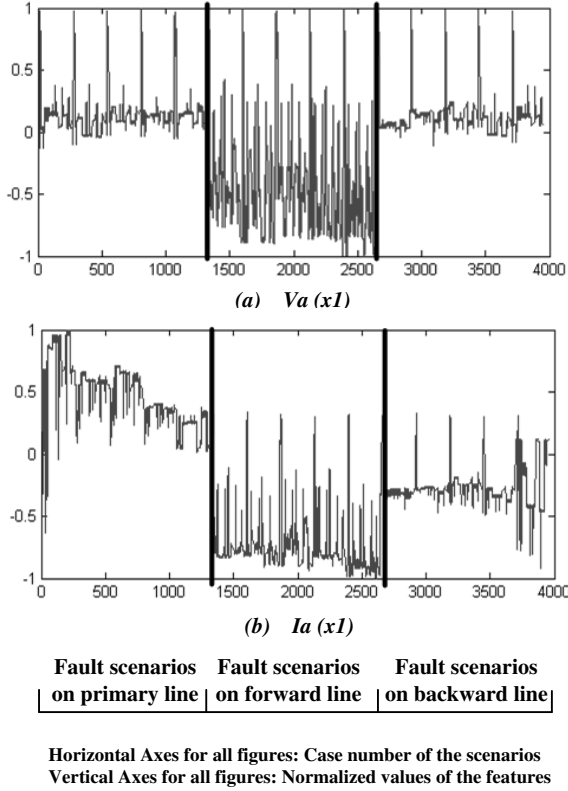


Fig. 11. Selected two features for generated 3960 cases

D. Performance Testing

We generated another 2000 fault scenarios for testing the protection schemes. There are 1000 fault cases on primary line and 500 for each of the other two lines. Those cases are selected from 15 fault points, including the six points shown in Fig. 8 and nine at other locations distributed along the three lines. The fault points are different from those in the training scenarios. For each fault point, other fault parameters are generated randomly for all fault types, fault resistances in the range of $0 - 100\Omega$, and fault angles in the range of $0 - 180^\circ$. The randomly generated scenarios may consist of some extreme cases and thus can demonstrate an overall statistical performance of the proposed scheme.

For boundary protection, the accuracy of fault detection is 99.7%. Among the six incorrect cases, only one involves the fault event on the primary line. For other five cases, the algorithm confuses the forward faults with the backward faults. Regarding fault type classification, only 1 of the 1000 cases is incorrect. The accuracy is 99.9%. The overall accuracy combining the boundary protection and fault classification can be calculated as $(1 - 7/2000) \times 100\% = 99.65\%$. Obviously, the overall performance of the proposed scheme is very good.

VII. DISCUSSION OF APPLICATION ISSUES

The previous section has evaluated the proposed protection scheme based on a typical system configuration. The real system may have different operating conditions and different system configurations from those of the test system used in the

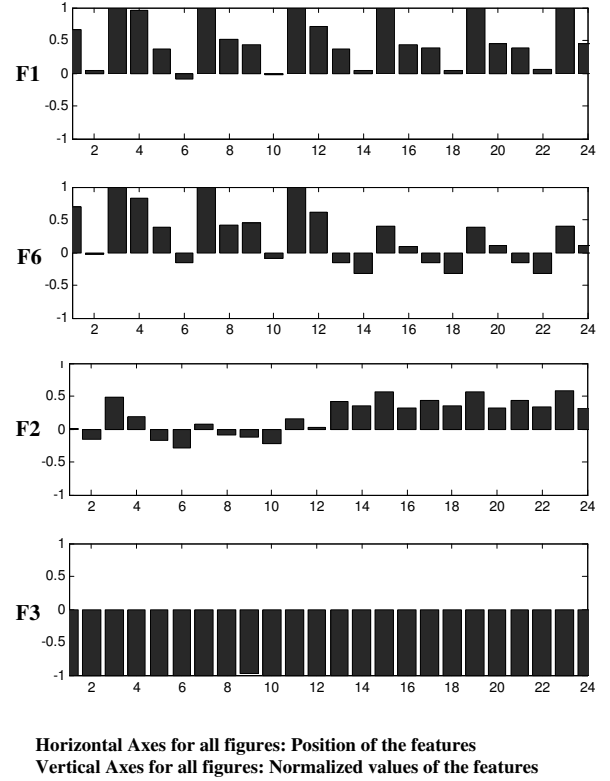


Fig. 12. Feature comparison faults close to the buses

last section. In order to give an overlook of the generality of the proposed scheme, this section will provide a discussion for other relevant issues based on more simulation results. Only boundary protection is considered since once the faulted section is located, fault classification using low frequency approximation of the fault signal is not difficult.

A. Fault and System Operating Conditions

1) *Faults close to the Bus*: Different fault parameters, fault types, fault locations, fault resistance and fault inception angles, have been included in the performance studies in last section. The test results using random scenarios show that the performance of the proposed scheme is less affected by those parameters. In an addition, it is interesting to examine the protection scheme performance for the faults occurring at the two sides close to the buses. Fig. 12 gives a feature comparison for those kinds of faults. Referring to the system shown in Fig. 8, four ABC faults at $F1$, $F6$, $F2$, and $F3$ with identical fault resistances and fault angles are simulated. This time the fault locations are placed directly behind the related buses. In Fig. 12, we can see the two pairs of faults directly at each side of the buses, $F1/F6$ and $F2/F3$, still have significant differences in the extracted features. Therefore, the proposed scheme will not have troubles in differentiating the internal faults close to the bus from the external ones.

2) *System Operating Conditions*: The simulations in Section VI are based on the normal system operating conditions. It is interesting to examine the proposed protection scheme during different loading conditions, topology changes due to

the line outages, etc. To simulate this effect, we generated four sets of scenarios. The loading conditions and line outages in other parts of the system can be emulated by adjusting the phase angle difference between the two sources. The original neural network is trained when the phase angle difference is 5° . Two sets of test scenarios are generated when the phase angle difference are 30° and 60° respectively. Another two sets of test scenarios correspond to the situations during the forward and reverse line outages respectively. For each test set, each line section has 100 fault scenarios which are randomly generated with different fault parameters. Note that the neural network is not retrained and it is exactly the one used in Section VI. The test results shown in Table I indicate that without retraining the neural network, the protection scheme still has good performance during different loading conditions and possible line outages in the system. When the line outage causes significant change of power flow patterns, the performance of the protection scheme will be somewhat influenced. For our studied system, the forward and reverse line outages are the most severe topological changes for the protection area. It would be better to store more than one set of trained neural networks to be able to respond to this kind of variance.

B. System Parameters

1) *Bus Capacitance*: The existence of bus capacitance in the high frequency band is the basic assumption for the proposed protection scheme. The value of the bus capacitance is the sum of the total capacitances of the equipment connected to the bus. The value selected in this paper is a typical one for EHV transmission system according to [2]. The real system may not have an exact bus capacitance as used in this paper since the size and design of different substations will be different. It is interesting to see how the proposed scheme responds or can be adjusted to different bus capacitances. Fig. 13 shows a feature comparison of two faults at $F2$ and $F3$ with other fault parameters identical in the system shown in Fig. 8. In Fig. 13 (a) the features are extracted when the bus capacitance is set as $0.1\mu F$ while Fig. 13 (b) are the features for bus capacitance of $0.05\mu F$. It is obvious that the latter case has worse feature difference than the former. If we increase the sampling rate to $500kHz$, the results are shown in Fig. 14. As shown in Fig. 14 (a), the feature difference for those faults with bus capacitance of $0.05\mu F$ is improved

TABLE I
TEST RESULTS FOR DIFFERENT SYSTEM OPERATING CONDITIONS

	DE(PL)	DE(FL)	DE(RL)	OA
PA- 30°	0/100	1/100	1/100	99.3%
PA- 60°	0/100	1/100	0/100	99.6%
FL-outage	0/100	-	6/100	97.0%
RL-outage	0/100	10/100	-	95.0%

DE: Detection Error (incorrect cases/total test cases)
OA: Overall Accuracy
PL: Primary Line; FL: Forward Line; RL: Reverse Line;
PA: Phase Angle Difference of Two Sources

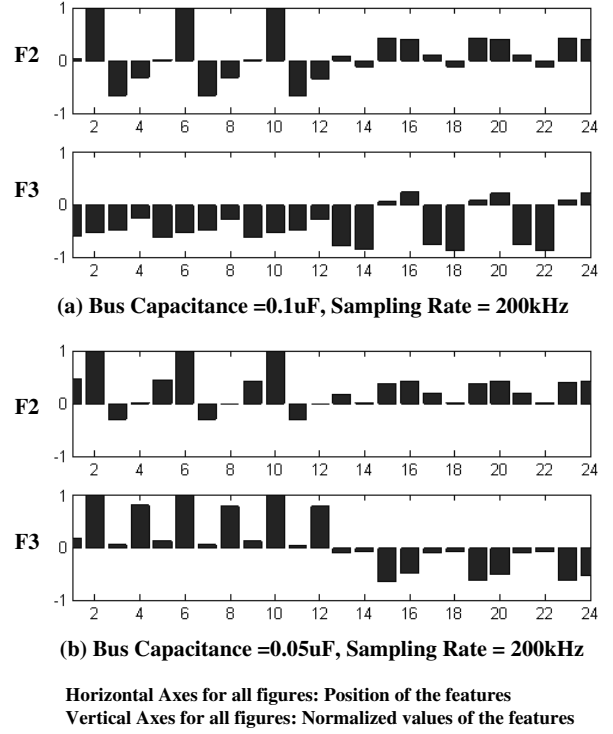


Fig. 13. Feature comparison for different bus capacitances (1)

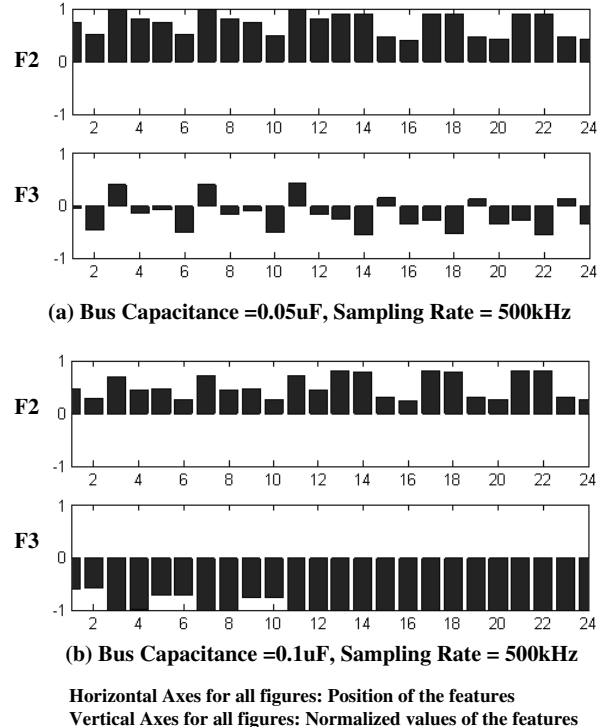


Fig. 14. Feature comparison for different bus capacitances (2)

significantly compared to Fig. 13 (b). The feature difference for bus capacitance of $0.1\mu F$ shown Fig. 14 (b) is also much better when compared to Fig. 13 (a).

The results lead to a conclusion that the higher bus capacitance affects less the proposed protection scheme. A minimum sampling frequency should be carefully selected to cope with the lowest bus capacitance in the protected area. If the bus capacitance is too low, line traps should be installed at the ends of the transmission lines to help refine the fault generated high frequency signals.

2) *Transmission Line Parameters*: The studied system in Section VI is a homogenous system. The three lines have identical length and parameters. They are all transposed. It is interesting to see the performance of the protection scheme in a less homogenous system. The original system shown in Fig. 8 is revised and shown in Fig. 15. In this system, the three lines are of different length. A section of a line of the length of 20 miles with different line parameters from the original lines is placed at the primary line and backward line, as shown in Fig. 15. Backward line and forward line are untransposed in this case. Using the same training and testing mechanism as introduced in Section VI, the test results are shown in Table II, where we can see that the variation of line parameters will not affect the performance of the proposed protection scheme. Similarly as in Fig. 11, we select two features from the training scenarios to compare the feature differences, as shown in Fig. 16. The features from different line sections are still generally distributed in different ranges. Although it is not as good as the cases in Fig. 11, the neural network based mechanism is still able to detect the faults from different line sections precisely.

C. System Structures

1) *Parallel Transmission Lines*: Parallel transmission lines are used in the transmission system due to their economic and environmental benefits. However, the protection of parallel lines are always challenging due to the mutual coupling effect of the two lines. This section will briefly study the proposed

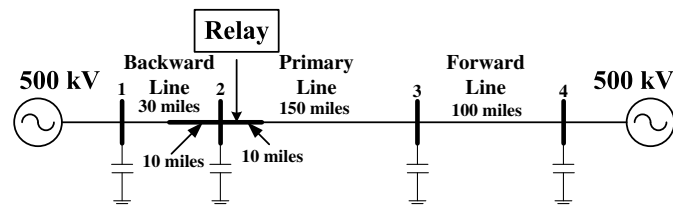


Fig. 15. The revised multi-line system

TABLE II
TEST RESULTS FOR NON-HOMOGENEOUS SYSTEM

DE(PL)	DE(FL)	DE(RL)	OA
0/100	1/100	0/100	99.7%

DE: Detection Error (incorrect cases/total test cases)
OA: Overall Accuracy
PL: Primary Line; FL: Forward Line; RL: Reverse Line;

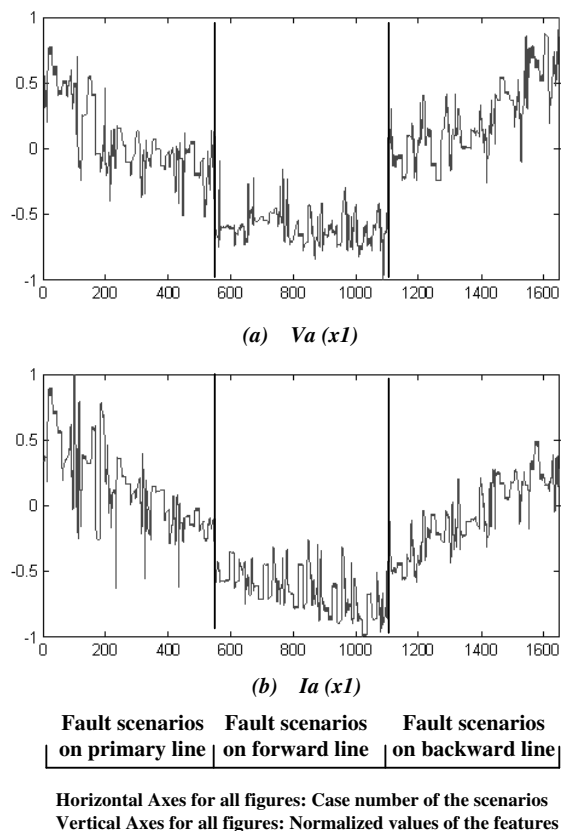


Fig. 16. Selected two features for training scenarios in non-homogeneous system

protection scheme when applied to the parallel lines. A test system with parallel lines is generated as shown in Fig. 17. This system has a strong source to the left with a source-to-line impedance ratio (SIR) of 0.5, and a weak source to the right with SIR=10. Generating fault scenarios and using the same training and testing mechanism as introduced in Section VI, the test results are shown in Table III. The performance is not as good as for the single lines. Select two features from the training scenarios to compare the feature differences, as shown in Fig. 18. It can be seen that the voltage features on both lines basically have same profiles. That means the detection depends

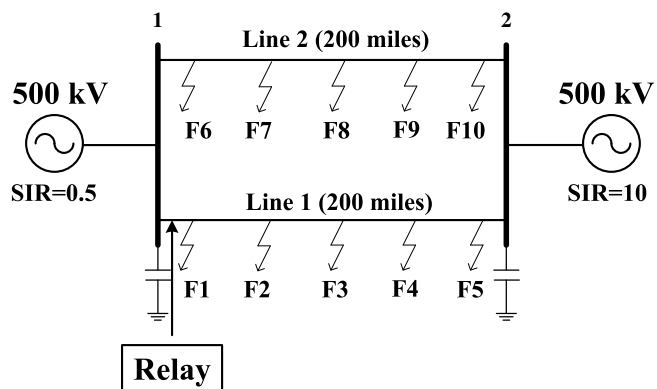
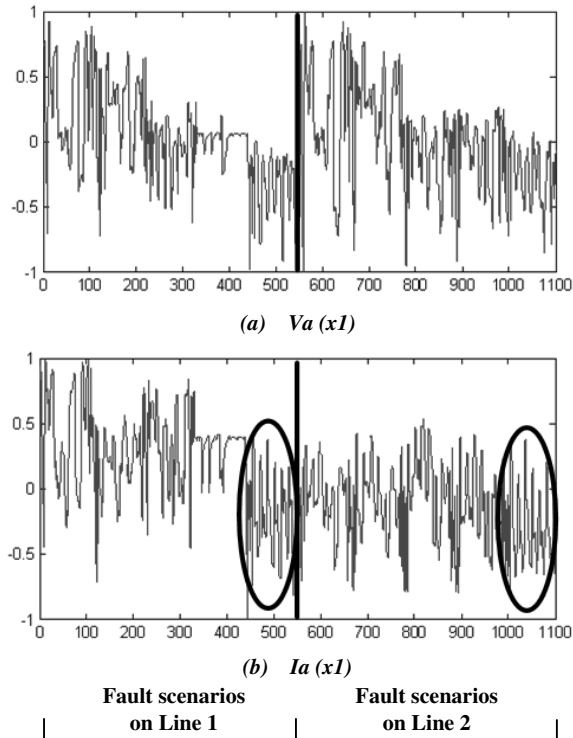


Fig. 17. The test system with parallel lines

TABLE III
TEST RESULTS FOR PARALLEL LINE SYSTEM

DE(L1)	DE(L2)	OA
3/100	13/100	92.0%

DE: Detection Error (incorrect cases/total test cases)
OA: Overall Accuracy
L1: Line 1; L2: Line 2;



Horizontal Axes for all figures: Case number of the scenarios
Vertical Axes for all figures: Normalized values of the features

Fig. 18. Selected two features for training scenarios in parallel line system

only on the current features. As shown in two circled areas in Fig. 18 (b), which corresponds to the faults at $F5$ and $F10$ respectively in the system shown in Fig. 17, the current profiles in this area are confusing each other and most of the detection errors come from those areas. The proposed protection scheme needs to be adjusted to deal with the parallel line protection. A possible solution is to install line traps at the each ends of both lines. The similar method can be found in [23]. This issue will be studied in detail in the future.

2) *Multi-terminal lines*: Multi-terminal lines are also used in the transmission system for economic and environmental benefits. It is not expected to have significant capacitances at the tap nodes in the multi-terminal systems. Therefore the basic assumption of the proposed approach may not exist in these systems. The application of the proposed protection scheme to such systems needs to be further studied.

As a summary for this section, the proposed approach has the generality for different fault and system operating conditions, as well as different system parameters. It needs to

be further studied and adjusted to cope with different system structures such as parallel lines and multi-terminal lines.

VIII. CONCLUSION

This paper is aimed at solving the problem of differentiating the internal faults from external ones using local-end data and providing the exact fault type at the same time. The paper applies advanced signal processing and artificial intelligence techniques to achieve that objective.

A comprehensive protection scheme is designed and the properties of the proposed scheme are:

- The signal preprocessing stage eliminates most of the influences from pre-fault loads, system conditions and power swings.
- The wavelet transform provides an efficient way to extract signal components at different frequency bands.
- The neural network provides an intelligent method and a “soft” criterion for feature comparison.
- Both high frequency details and low frequency approximations are being used in the proposed method and that can avoid confusing faults with other kinds of non-fault disturbances.
- The protection tasks are distributed into two neural networks so that each neural network has different task.
- Both neural networks take half cycle data window, therefore the protection speed is satisfied.
- To be able to cope with specific system structures such as parallel lines and multi-terminal lines, more adjustments are needed.

REFERENCES

- [1] Z. Q. Bo, F. Jiang, Z. Chen, X. Dong, G. Weller, and M. A. Redfern, “Transient based protection for power transmission systems,” in *Proc. IEEE PES Winter Meeting*, Singapore, Jan. 2000, vol. 3, pp. 1832–1837.
- [2] Z. Q. Bo, “A new non-communication protection technique for transmission lines,” *IEEE Trans. Power Delivery*, vol. 13, no. 4, pp. 1073–1078, Oct. 1998.
- [3] A. T. Johns and P. Agrawal, “New approach to power line protection based upon the detection of fault induced high frequency signals,” *IEE Proc. on Generation, Transmission and Distribution*, vol. 137, no. 4, pp. 307–313, July 1990.
- [4] V. Pathirana and P. G. McLaren, “A hybrid algorithm for high speed transmission line protection,” *IEEE Trans. Power Delivery*, vol. 20, no. 4, pp. 2422–2428, Oct. 2005.
- [5] X. N. Lin, Z. Q. Bo, B.R.J. Cauce, and N. F. Chin, “Boundary protection using complex wavelet transform,” in *Proc. Sixth International Conf. on Advances in Power System Control, Operation and Management*, Hong Kong, Nov. 2003, vol. 2, pp. 744–749.
- [6] A. G. Phadke and J. S. Thorp, *Computer Relaying for Power Systems*, Wiley, Taunton, United Kingdom, 1988.
- [7] S. Vasilic and M. Kezunovic, “Fuzzy ART neural network algorithm for classifying the power system faults,” *IEEE Trans. Power Delivery*, vol. 20, no. 2, pp. 1306–1314, Apr. 2005.
- [8] R. K. Aggarwal, A. T. Johns, Y. H. Song, R. W. Dunn, and D. S. Fitton, “Neural-network based adaptive single-pole autoreclosure technique for EHV transmission systems,” *IEE Proc. on Generation, Transmission and Distribution*, vol. 14, no. 2, pp. 155–160, Mar. 1994.
- [9] C. H. Kim and R. Aggarwal, “Wavelet transforms in power systems Part 1: General introduction to the wavelet transforms,” *Power Engineering Journal*, vol. 14, no. 2, pp. 81–88, Apr. 2000.
- [10] C. H. Kim and R. Aggarwal, “Wavelet transforms in power systems Part 2: Examples of application to actual power system transients,” *Power Engineering Journal*, vol. 15, no. 4, pp. 193–202, Aug. 2001.
- [11] S. Santoso, E. J. Powers, W. M. Grady, and P. Hofmann, “Power quality assessment via wavelet transform analysis,” *IEEE Trans. Power Delivery*, vol. 11, no. 2, pp. 924–930, Apr. 1996.

- [12] A. H. Osman and O. P. Malik, "Transmission line distance protection based on wavelet transform," *IEEE Trans. Power Delivery*, vol. 19, no. 2, pp. 515–523, Apr. 2004.
- [13] O. Youssef, "New algorithm to phase selection based on wavelet transforms," *IEEE Trans. Power Delivery*, vol. 17, no. 4, pp. 908–914, Oct. 2002.
- [14] *Wavelet Toolbox User's Guide*, The MathWorks Inc., Natick, MA, June 2005. [Online] <http://www.mathworks.com/>
- [15] M. Kezunovic, "A survey of neural net application to protective relaying and fault analysis," *Engineering Intelligent Systems*, vol. 5, no. 4, pp. 185–192, Dec. 1997.
- [16] T. S. Sidhu, H. Singh, and M. S. Sachdev, "Design, implementation and testing of an artificial neural network based fault detection discriminator for protecting transmission lines," *IEEE Trans. Power Delivery*, vol. 10, no. 2, pp. 697–706, Apr. 1995.
- [17] D. S. Fitton, R. W. Dunn, R. K. Aggarwal, A. T. Johns, and A. Bennett, "Design and implementation of an adaptive single pole autoreclosure technique for transmission lines using artificial neural networks," *IEEE Trans. Power Delivery*, vol. 11, no. 2, pp. 748–756, Apr. 1996.
- [18] G. A. Carpenter and S. Grossberg, "ART2: Self-organization of stable category recognition codes for analog input patterns," *Applied Optics*, vol. 26, no. 23, pp. 4919–4930, Dec. 1987.
- [19] J. Keller, M. R. Gray, and J. A. Givens, "A fuzzy K-nearest neighbor algorithm," *IEEE Trans. Systems, Man and Cybernetics*, vol. 15, no. 4, pp. 580–585, July/Aug. 1985.
- [20] Y. Ge, *New Types of Protective Relaying and Fault Location Theory and Techniques*, Xi'an Jiaotong University Press, Xi'an, China, 1993.
- [21] CanAm EMTP UG (2002), Alternative Transients Program. [Online] <http://www.emtp.org/>
- [22] *Using MATLAB*, The MathWorks Inc., Natick, MA, Aug. 2002. [Online] <http://www.mathworks.com/>
- [23] Z.Q. Bo, R.K. Aggarwal, and A.T. Johns, "Non-unit protection of double circuit lines based on fault generated high frequency signals," in *Proc. IEE 2nd International Conf. on Advances in Power System Control, Operation and Management*, Hong Kong, Dec. 1993, pp. 77–82.



Nan Zhang (S'04) received his B.S. and M.S. degrees from Tsinghua University, Beijing, China both in electrical engineering, in 1999 and 2002 respectively. Since Jun. 2002, he has been with Texas A&M University pursuing his Ph.D. degree. His research interests are power system analysis, power system protection, power system stability, system-wide disturbances, as well as signal processing and artificial intelligence applications in power systems.



Mladen Kezunovic (S'77, M'80, SM'85, F'99) received his Dipl. Ing. degree, the M.S. and Ph.D., all in electrical engineering, in 1974, 1977 and 1980, respectively. Dr. Kezunovic's industrial experience is with Westinghouse Electric Corporation in the USA, and the Energoinvest Company in Europe. He was a Visiting Associate Professor at Washington State University in 1986-1987. He has been with Texas A&M University since 1987 where he is the Eugene E. Webb Professor and Director of Electric Power and Power Electronics Institute. His main research interests are digital simulators and simulation methods for equipment evaluation and testing as well as application of intelligent methods to control, protection and power quality monitoring. Dr. Kezunovic is a registered professional engineer in Texas, and a Fellow of the IEEE.